To link to this article: DOI: 10.1016/j.neuroimage.2012.12.060
URL: http://dx.doi.org/10.1016/j.neuroimage.2012.12.060

To cite this version: Causse, Mickael and Péran, Patrice and Dehais, Frédéric and Caravasso, Chiara Falletta and Zeffiro, Thomas and Sabatini, Umberto and Pastor, Josette *Affective decision making under uncertainty during a plausible aviation task: An fMRI study.* (2013) NeuroImage, vol. 71. pp. 19-29. ISSN 1053-8119

Affective decision making under uncertainty during a plausible aviation task: an fMRI study

Mickaël Causse[1, 2], Patrice Péran[2, 3], Frédéric Dehais[1], Chiara Falletta Caravasso[3], Thomas Zeffiro[4], Umberto Sabatini[3], Josette Pastor[2]

[1]Institut Supérieur de l'Aéronautique et de l'Espace, Département Mathématiques, Informatique, Automatique; Université de Toulouse; 10 avenue E. Belin 31055 Toulouse Cedex 4, France
[2]Inserm; Imagerie cérébrale et handicaps neurologiques UMR 825; F-31059 Toulouse, France
Université de Toulouse; UPS; Imagerie cérébrale et handicaps neurologiques UMR 825; CHU Purpan, Place du Dr Baylac, F-31059 Toulouse Cedex 9, France
[3]Radiology Department, IRCCS Santa Lucia Foundation, via Ardeatina 306, Rome, 00149, Italy
[4]Neural Systems Group, CNY 149, Massachusetts General Hospital, Boston, Massachusetts, USA

Abstract

In aeronautics, plan continuation error (PCE) represents failure to revise a flight plan despite emerging evidence suggesting that it is no longer safe. Assuming that PCE may be associated with a shift from cold to hot reasoning, we hypothesized that this transition may result from a large range of strong negative emotional influences linked with the decision to abort a landing and circle for a repeat attempt, referred to as a "go-around". We investigated this hypothesis by combining functional neuroimaging with an ecologically valid aviation task performed under contextual variation in incentive and situational uncertainty. Our goal was to identify regional brain activity related to the sorts of conservative or liberal decision-making strategies engaged when participants were both exposed to a financial payoff matrix constructed to bias responses in favor of landing acceptance, while they were simultaneously experiencing maximum levels of uncertainty related to high levels of stimulus ambiguity. Combined with the observed behavioral outcomes, our neuroimaging results revealed a shift from cold to hot decision making in response to high uncertainty when participants were exposed to the financial incentive. Most notably, while we observed activity increases in response to uncertainty in many frontal regions such as dorsolateral prefrontal cortex (DLPFC) and anterior cingulate cortex (ACC), less overall activity was observed when the reward was combined with uncertainty. Moreover, participants with poor decision making, quantified as a lower discriminability index d', exhibited riskier behavior coupled with lower activity in the right DLPFC. These outcomes suggest a disruptive effect of biased financial incentive and high uncertainty on the rational decision-making neural network, and consequently, on decision relevance.

Keywords: reward and punishment, dorsolateral prefrontal cortex, risk-taking, emotion, aviation safety

1. Introduction

Functional brain imaging allows investigation of the neural mechanisms underlying phenomena that occur during complex real life activities. Examples are seen in aeronautics research, where different studies have identified specific neural activity patterns (Callan, et al., 2012; Caldwell et al., 2005; Menda et al., 2011; Peres et al., 2000) or regional brain volume variations related to piloting performance (Adamson et al., 2010). Results from these studies can indicate possible causal factors related to accidents, may be helpful in refining pilot selection and training criteria, and can assist safety boards in developing policy recommendations for airlines. Functional neuroimaging methods could be particularly useful in understanding the neural mechanisms underlying plan continuation error (PCE), known as failure to revise a flight plan despite emerging evidence suggesting that it is no longer safe (Orasanu, Ames, Martin, & Davison, 2001). In such risky situations, the pilot may decide to perform a go-around or execute a diversion if indicated. However, a famous study conducted at MIT (Rhoda & Pawlak, 1999) demonstrated that, in 2000 cases of approaches performed under thunderstorm conditions, two aircrews out of three continued the flight plan and erroneously persisted with approach and landing. While several cognitive theories have been proposed to explain this result (Causse, Dehais, Arexis, & Pastor, 2011; Causse, Dehais, & Pastor, 2011; Goh & Wiegmann, 2002), it may be that PCE is favored by strong negative emotions associated with the decision to revise the flight plan. These negative emotional consequences could adversely alter a pilot's rational reasoning by biasing decision-making criteria, thereby unconsciously affecting their risk assessments and the subsequent course of action chosen. Indeed, a forced go-around, by increasing uncertainty and destabilizing the pilot's emotional state, may lead to great difficulties in reinserting the aircraft back in the traffic pattern. Moreover, a go-around has important financial consequences for airlines due to its attendant extra fuel consumption. One now defunct airline formerly paid passengers one dollar for each minute their flight was late, until a crew attempted to land through a thunderstorm and crashed (Nance, 1986). It is assumed that pilots frame their decision to continue landing in terms of potential losses (O' Hare & Smitheram, 1995), such as increased anxiety, money spent on fuel consumption, or flight delays. In this context, pilots may be willing to take safety risks to avoid possible losses related to late arrival. Indeed, Kahneman and Tversky's behavioral economical theory (1979) demonstrated that people are particularly biased towards risk taking when faced with the prospect of losses.

It is widely accepted that emotion can jeopardize decision-making relevance or risk assessment, especially in highly uncertain situations (Damasio, 1994) and during complex tasks that involve dorsolateral prefrontal cortex (DLPFC) and anterior cingulate cortex (ACC) (Qin, Hermans, van Marle, Luo, & Fernández, 2009; Schoofs, Preuss, & Wolf, 2008). Neuroeconomic studies have explored the effects of monetary reward and punishment on cognition. For instance, Taylor et al. (2004) highlighted the efficiency of financial incentive in biasing working memory and object recognition. Dreher, Kohn, & Berman (2006) found that reward can hasten decision-making processes. The DLPFC is involved in reasoning and its activity is related to reduced risk-taking behavior (Knoch, et al., 2006) and reward probability (Dreher, et al., 2006). However, orbitofrontal cortex (OFC), which participates in emotion processing, modulates the anticipation of regret linked to financial loss (Coricelli et al., 2005). Other work has introduced the concept of 'hot' and 'cold' reasoning (Goel & Dolan, 2003; Schaefer et al., 2003), where 'hot' reasoning refers to modulation of reasoning by emotion and 'cold' reasoning is considered more purely cognitive. Therefore, manipulation of rewards and punishments may interfere both with cognition and emotion, suggesting that a parallel could be drawn between neuroeconomic study tasks and the decision making contexts in which pilots are placed in conflict between conditions of punishment, involving extra fuel consumption or fatigue caused by a second landing attempt, and reward, involving delivering passengers without delay.

Our hypothesis is that PCE may be a consequence of a shift from cold to hot reasoning. This transition may result from a large range of strong negative emotional consequences linked with the decision to undertake a go-around when uncertainty is high. In this perspective, hot reasoning is less rational from a safety viewpoint and integrates modulatory emotional influences. In this study, we investigated this hypothesis with a simplified, but plausible, landing task based on the standard cockpit instrument landing system (ILS), using functional magnetic resonance imaging (fMRI) to estimate changes in brain activity related either to the type of incentive (neutral or financial) or the level of uncertainty (low or high). Our analysis focused on identifying brain regions involved in decision-making (conservative vs. liberal strategies) when participants were both exposed to a financial payoff matrix, constructed to bias responses in favor of landing acceptance, under conditions of maximum levels of uncertainty induced by high stimulus ambiguity.

2. Methods

2.1. Participants

Fifteen young physically and psychiatrically healthy participants were recruited from the local community to participate in the experiment (mean age = 25.4 years, SD = 2.45; mean education level = 16.68 years of schooling, SD = 1.95). All were right-handed as measured using the Edinburgh handedness inventory (Oldfield, 1971). Due to their influence on decision-making processes, emotional profiles were quantified using impulsivity and anxiety assessments with the Italian version of the Barratt Impulsiveness Scale (BIS-11) (Fossati, Di Ceglie, Acquarini, & Barratt, 2001) and the Italian version of the Spielberger Trait Anxiety Inventory (STAI form Y-2) (Spielberger, Pedrabissi, & Santinello, 1996). Impulsivity was estimated from the mean of the motor, cognitive and non-planning impulsivity subscales. Both impulsivity and trait anxiety levels were within the normal range for all participants (Fossati, et al., 2001; Spielberger, et al., 1996) (respectively, mean = 60.50, SD = 8.95; mean = 41.50, SD = 4.03). Participants gave informed consent before participation. They were paid and were told that they would earn extra money according to their task performance. Participants were also told that they would earn a percentage of the amount of money presented on the screen after each response. Eventually, for ethical reasons, all participants won the maximum amount of money.

2.2. Experimental paradigm

We used a 2x2 factorial design crossing two independent variables, financial incentive and uncertainty. The task was based on simplified reproduction of a real flight instrument featuring a 480x480 pixel display. This instrument supports the pilot's decision-making during landing without external visibility. Participants were instructed that they would be flying a plane that had reached the decision altitude, that is, the point of the approach where the pilot must decide if the landing has to be aborted or not. At that time they would be allowed to defer landing if they believed that it was unsafe. Decisions were based on two elements of the ILS: localizer and glide, which respectively provide lateral and vertical guidance to adjust the trajectory of the aircraft relative to the runway. The information was given by two rhombi, displayed below and on the right of the artificial horizon, as in a real aircraft (Figure 1).

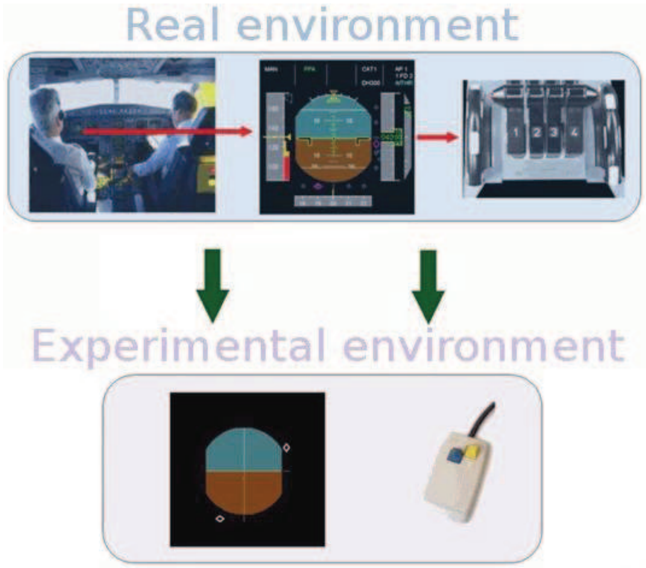

Figure 1. Simplified reproduction of the decision-making environment during the landing phase. In the upper part, the real environment. From left to right: the real cockpit, a zoomed view of the main instrument panel showing the ILS and the throttle. In the bottom part, the experimental environment is shown. From left to right are shown: the simplified main instrument with only the two rhombi of the ILS (in white) and the response pad using to signal the results of the decision to land or to perform a go-around.

Participants were reminded that landing was safe when both rhombi were close to the center of their respective axis and that as the rhombi moved farther from the center, the risk of crash increased. Participants were asked to be aware of the great importance of flight safety. Landing situations were manipulated according to low and high levels of uncertainty, indexed by the level of information ambiguity provided by the ILS instrument (Figure 2).

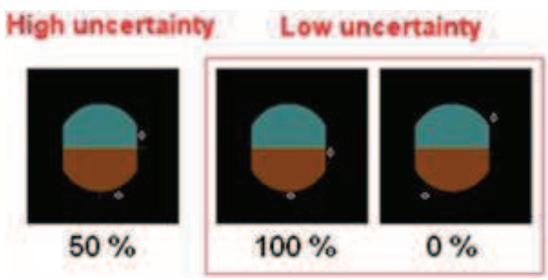

Figure 2. Categorization of the level of uncertainty according to the rhombus positions. The rhombi positions were counterbalanced to avoid laterality effects. The order of presentation of the stimuli was randomized for each run.

In the landing condition without uncertainty, decision making was straightforward: either the rhombi were very far from their respective centers, requiring a go-around (likelihood of successful landing: 0%), or they were very close, requiring landing acceptance (likelihood of successful landing: 100%). In landing conditions with high uncertainty, rhombi had borderline positions (not very far or very close to the center) and the likelihood (unknown to the participants) of a successful landing or a crash, was 50%. Within a run, there was no repetition of the same rhombus pattern. These changes in uncertainty level reduced stimulus habituation and promoted a sustained high level of reasoning throughout the experiment.

Two runs (1 run = 40 trials) were presented in each condition: neutral or financial. For each trial, the participants indicated their choice (landing or no landing) by pressing a button on the response pad. After each response, the participants received feedback concerning response accuracy (OK, for a successful landing or a justified go-around; NO, for an erroneous decision to land or an unjustified go-around). During the financial incentive condition, negative emotional consequences associated with a go-around were induced using a visual payoff matrix (Figure 3). In the high uncertainty condition, feedback (successful landing or crash) was randomized.

Figure 3. The various feedback screens displayed after each decision. Without incentive, only the accuracy feedback was delivered (OK/NO), with financial incentive, the monetary consequences were also displayed after the accuracy feedback.

This payoff matrix was designed to bias responses in favor of landing acceptance. A go-around was systematically punished with a financial penalty. The penalty was less important (-2€) when the go-around was justified than when it was unjustified (-5€). This systematic punishment of the decision to go-around reproduced the sorts of systematic negative consequences encountered in real life. While successful landing was rewarded (+5€), an erroneous decision to land was punished (-2€). While the fact that the erroneous decision to go-around was more severely punished than the erroneous decision to land may appear counterintuitive, the matrix was constructed in this way for several reasons. First, during real flights, pilots know that crash and overrun are rather unlikely events, whereas the negative consequences associated with a go-around are systematic. The analysis of unstabilized approaches confirms that accidents are rather rare in spite of frequent risk taking (Rhoda & Pawlak, 1999). Interestingly, Kahneman and Tversky (1979) demonstrated that people are particularly risk seeking when faced with the prospect of losses. Second, introducing very rare events would have been problematic since low numbers of repetitions of given experimental conditions might not provide sufficient statistical power to detect the regional effects of interest. For these reasons, we were compelled to modulate the weight of the punishment rather than its frequency. At the end of each run, a global feedback "safety score" display indicated the percentage of correct responses. Moreover, at the end of the financial run, a "financial score" feedback indicated the cumulative amount of money won or loss. These two scores are in conflict since the optimization of the "financial score" can only be achieved at the expense of the safety score as it necessarily implies a dangerous increase in the landing acceptance rate.

2.3. Stimuli presentation

Stimulus display and data acquisition were controlled with Cogent 2000 v125 and MATLAB (Matlab R2006a, The MathWorks, USA). Each trial (Figure 4) consisted of presentation of the stimulus for 2.5 s, during which time the participant signaled a decision by making a response, followed by a variable delay of 6-10 s, followed by the appearance of the response accuracy feedback display for 2 s. During the incentive condition, accuracy information was displayed for 0.5 s, followed by financial outcome (+5€, -5€ or –2€) for 1.5 s. Finally, this was followed by a variable inter-trial interval (ITI) of 3-9 s. The long delay before feedback allowed us to distinguish the activity associated with decision making during the stimulus presentation from the sustained activity associated with reward expectancies during the delay period. The 3-9 s fixation period between trials constituted an implicit baseline condition. Before the experiment, participants practiced one neutral and one financial run to become familiar with the task and the payoff matrix.

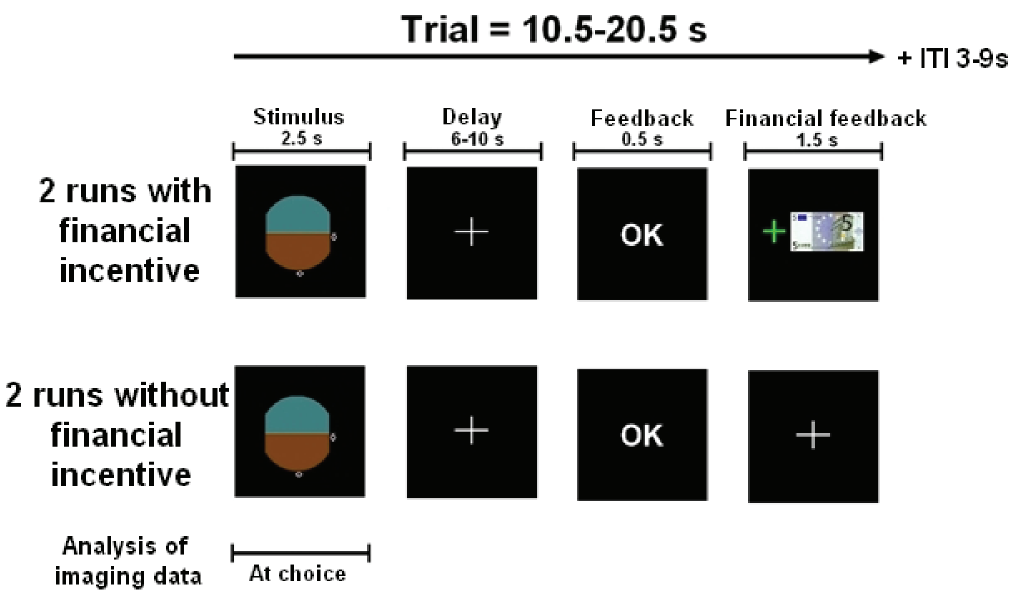

Figure 4. Illustration of the stimuli during the two types of experimental runs: financial and neutral. The order in which the runs were performed was counterbalanced across participants.

2.4. fMRI data acquisition and analysis

The experiment was conducted at the Radiology Department of the Santa Lucia Foundation (Rome). All the data were acquired in a single session on a 3 Tesla Allegra MRI system (Siemens Medical Solutions, Erlangen, Germany) with a maximum gradient strength of 40 mT/m. We used a standard quadrature birdcage head coil for both RF transmission and reception. The fMRI data were acquired using gradient echo EPI, with 38 axial slices and a voxel size of 3.0 × 3.0 × 3.75 mm (matrix size 64 × 64; FOV 192 × 192 mm) in ascending order; repetition time 2.47 s; and flip angle 90°. Data analysis was performed with SPM8 (Wellcome Trust Centre for Neuroimaging, London, UK). First, data were slice time corrected using sinc interpolation and then realigned to correct head motion. A mean functional image volume was computed from the realignment step and these mean images were normalized to the SPM8 Montreal Neurological Institute (MNI) EPI template with affine registration followed by nonlinear transformation. The normalization parameters determined for the mean functional volume were then applied to the corresponding functional image volumes. Finally, images were smoothed with an 8 mm^3 isotropic Gaussian smoothing kernel. Each participant's spatially normalized image set was analyzed with a general linear model, using 12 experimental regressors, a 128 sec high-pass filter, 3 events (at choice, at delay, and at feedback) x 4 conditions per event (level of uncertainty * type of incentive), each convolved with a canonical hemodynamic response function. For each participant, the four experimental conditions were contrasted with the implicit fixation baseline. At the second level, individual images of contrast parameters were entered into a mixed-effects repeated measures, factorial model with three factors, subject, incentive (two levels), and uncertainty (two levels).

All planned analysis focused on the decision making period ("at choice') in each trial, (Figure 4). Contrasts were calculated for uncertainty (high vs. low) and incentive (financial vs. neutral) as main effects along with their associated interaction terms. To obtain anatomical labels, the location of activity peaks were summarized as local maxima and then converted from MNI to Talairach coordinate space using an MNI-to-Talairach transformation algorithm (Lancaster et al., 2007). These coordinates were used to determine the nearest gray matter label using the Talairach Daemon version 2.4.2 (Lancaster et al., 2000) and were reported in Talairach space. Statistical parametric maps were overlaid onto a reference brain using xjview (http://www.alivelearn.net/xjview8/).

For examination of the task vs. baseline effects for high uncertainty in a neutral context ([Neutral_High]), the critical threshold significance was set at $p < 0.0001$ with FDR correction at the whole-brain level. For additional protection against false-positives, only clusters > 337.5 mm^3 (10 voxels) are reported. We next examined the weaker between-condition effects at $p < 0.005$, not corrected for multiple comparisons. Last, we used small volume correction (SVC) with multiple comparisons controlled at $p < 0.05$ (family-wise error) for *a priori* anatomical ROIs previously found to be modulated consistently in previous functional neuroimaging studies of decision-making under uncertainty and reward processing (Callan, et al., 2009; Coricelli et al., 2005; Platt & Huettel, 2008; Qin, et al., 2009; Rauss, Pourtois, Vuilleumier, & Schwartz, 2012). These regions were identified using anatomical masks created using the WFU PickAtlas Tool, Version 2.4 (Maldjian, Laurienti, Kraft, & Burdette, 2003) and included medial prefrontal gyrus (BA6), DLPFC (BA9), ACC (BA 24 and 32), OFC (BA 11 and 47), the striatum, and visual cortex (BA17, BA18, BA19). A separate mask was created for each ROI, and small volume searches were performed for each region. Effect sizes (Cohen's D) were calculated by transforming *t*-maps into effect size maps using the

SPM8 Volumes Toolbox. Clusters exceeding a threshold of $p < 0.005$ (uncorrected for multiple comparisons) at the whole-brain level are also reported.

2.5. Behavioral data analysis

All behavioral data were analyzed with Statistica 7.1 (StatSoft ©). Mean response times (RT) and percentage of landing acceptance were calculated for each experimental condition. The effects of the type of incentive (neutral vs. financial) and the level of uncertainty on RT and the percentage of landing acceptance were examined with a two-way 2 * 2 (type of incentive * level of uncertainty) repeated measures ANOVA. Tukey's honestly significant difference (HSD) *post hoc* test was used to examine paired comparisons. In order to further analyze neural activity relationships with behavior, we then calculated an individual discriminability index (d') with signal detection theory equations for the financial condition with high uncertainty. This metric give a reliable indicator on participant's decision-making criterion which is the standardized difference between hit rate and false alarm rate distributions.

3. Results

3.1. Behavioral results

Reaction times

Repeated measures ANOVA revealed a main effect of uncertainty on RT ($F(1, 15) = 40.25$, $p < 0.001$, $\eta^2_p = .73$). High uncertainty generated longer mean RT compared to low uncertainty (respectively: 1223 ms, SE = 60.90; 980 ms, SE = 35.09). In addition, the

ANOVA revealed a main effect of the type of incentive on the RT ($F(1, 15) = 13.58$, $p = 0.002$, $\eta^2_p = .48$). During the financial condition, RTs were shorter than during the neutral condition (respectively: 1064 ms, SE = 41.40; 1139 ms, SE = 51.94). There was an interaction between the level of uncertainty and the type of incentive ($F(1, 15) = 9.19$, $p = 0.008$, $\eta^2_p = .38$). When uncertainty was high, participants were quicker to make a decision under the financial pressure (HSD < 0.001), whereas RTs remained quite stable when uncertainty was low (HSD = 0.985).

Landing acceptance and discriminability index d'

The magnitude of the mean total outcome was positive (+34.5€, SD = 57.7), confirming that the reward biased decision making toward economic optimization. A perfectly unbiased decision would have led participants to receive a markedly negative outcome (-140€). We first roughly calculated the overall proportion of landing acceptance for each of the four experimental conditions. The ANOVA showed that there was a main effect of the type of incentive ($F(1,15) = 57.41$, $p < 0.001$, $\eta^2 p = .79$) and level of uncertainty ($F(1,15) = 19.93$, $p < 0.001$, $\eta^2 p = .57$) on landing acceptance. An incentive * level of uncertainty interaction was also found ($F(1,15) = 5.07$, $p = 0.039$, $\eta^2 p = .27$), showing that the effect of the financial incentive only occurred when uncertainty was high (HSD < 0.001). The higher landing acceptance rate occurred during the financial with high uncertainty condition. As expected, in response to the asymmetric payoff matrix, participants exhibited a significant shift in the likelihood of making an affirmative response. The shift meant that participants were willing to experience higher false alarms (land in a go-around stimulus) to achieve more hits and avoid miss (go-around in a landing stimulus). This shift was the intended result of the payoff matrix, set up to bias responses with financial incentive and high uncertainty. In accordance with our expectations, the lower d' was found during the rewarded condition with high uncertainty

(2.51, SD = 0.72). Whereas the financial incentive did not affect d' index in the neutral condition (p = 0.966), the introduction of the reward/penalty system affected d' index in the highly uncertain context ($F(1,14) = 8.79$, $p = 0.010$, $\eta^2 p = .38$).

3.2. Neuroimaging results

Task effect

We first identified the voxels that were active at choice with high uncertainty in neutral context ([Neutral_High]) versus rest condition. This analysis allowed us to examine the overall effect of task on brain activity. Table 1 summarizes these results. Notably, activity foci were found in frontal regions including the DLPFC and the ACC. Activity in the insula and the thalamus was also observed, see Figure 5.

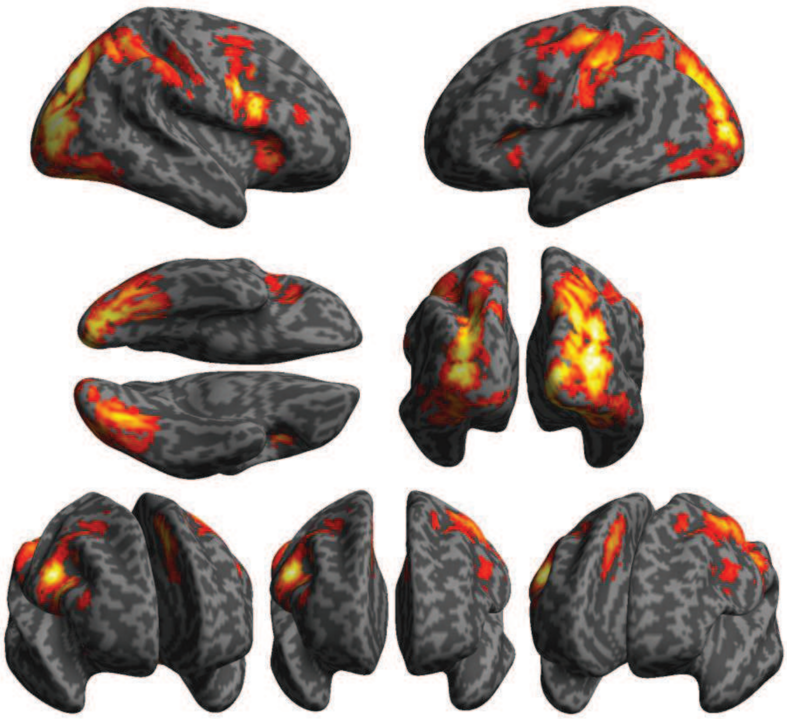

Figure 5. The main task effect was examined by contrasting the high uncertainty condition in the neutral context against the implicit baseline. Notably, the figure shows foci of activity in the right DLPFC, the ACC and visual cortex, with activity peaks in the middle occipital gyrus.

Table 1. Task effect revealed by contrasting the high uncertainty condition in the neutral context against the implicit baseline. Activity peaks occurring in clusters of ten or more contiguous voxels ($p < 0.0001$ FDR) are reported. [a]Cohen's D measure of effect size

Brain regions	Side	BA	Talairach Coordinates			*t*-score	z	Effect size[a]	k
			x	y	z				
Inferior frontal gyrus (DLPFC)	L	9	-48	6	28	9.48	6.89	2.80	57
	R	9	48	9	25	20.68	∞	6.24	445
	R	47	33	25	0	13.08	∞	3.94	157
Anterior cingulate gyrus	R	32	6	21	38	14.39	∞	4.33	504
Middle occipital gyrus	R	19	33	-79	21	19.63	∞	6.02	4381
Insula	L	13	-33	17	8	12.66	∞	3.81	68
	R	13	33	22	3	10.42	7.28	3.56	101
Thalamus	L	N/A	-9	-15	7	10.45	7.30	3.15	28
	R	N/A	9	-12	7	9.06	6.71	2.74	11

Main effects of the high level of uncertainty

We examined the main effect of the high vs. low uncertainty with an analysis that included both types of incentive ([High vs. Low]). Notably, decision making under high uncertainty was associated with increased anterior activity, in DLPFC, ACC, and medial frontal gyrus (premotor cortex). Parietal (superior parietal lobule) as well as occipital cortices also showed enhanced activity. In addition, bilateral activity was observed in the putamen (Figure 6 and Table 2). The opposite contrast ([Low vs. High]) yielded no significant effects.

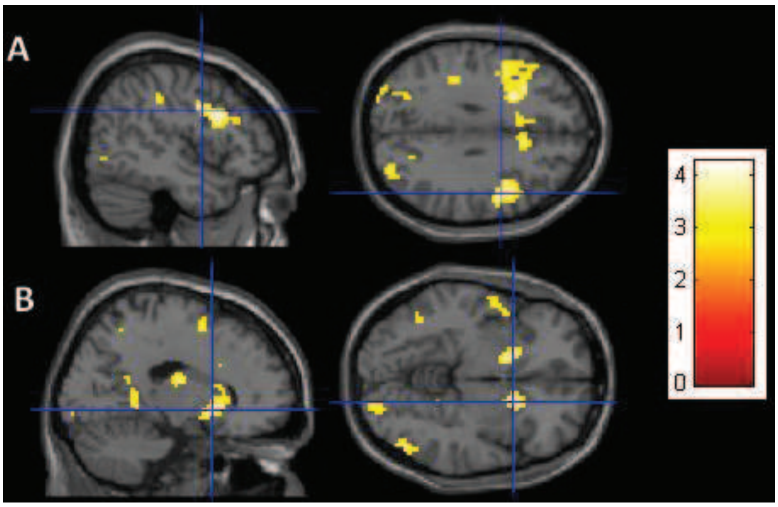

Figure 6. Main effect of high vs. low uncertainty. (A) Foci of activity in the right DLPFC and in the (B) putamen. Both foci survived SVC, $p < 0.05$ FWE.

Table 2. Main effects of high vs. low uncertainty in activity peaks from clusters of ten or more contiguous voxels ($p < 0.005$ uncorrected). [a]Cohen's D measure of effect size. [b]Survived SVC ($p < 0.05$ FWE).

Brain regions	Side	BA	Talairach Coordinates			*t*-score	z	Effect size[a]	k
			x	y	z				
Middle frontal gyrus	L	10	-39	46	10	2.96	2.81	0.90	18
	R	8	27	16	44	2.90	2.46	0.89	10
Inferior frontal gyrus (DLPFC)	L	9	-33	6	25	3.19	3.00	1.07	80
Inferior frontal gyrus (DLPFC)[b]	R	9	46	15	22	4.26	3.86	1.28	272
Anterior cingulate gyrus[b]	R	24	9	21	25	4.00	3.66	1.20	48
Anterior cingulate gyrus	L	32	-6	19	41	3.59	3.33	1.08	42
Medial frontal gyrus	L	6	-21	4	48	4.25	3.86	1.28	16
	R	6	21	4	50	3.69	3.42	1.06	24
Postcentral gyrus	R	2	50	-28	38	3.45	3.22	1.03	23
Superior parietal lobule	L	7	-24	-63	40	3.86	3.55	1.18	168
Middle temporal gyrus	L	37	-45	-59	1	3.22	3.02	0.97	20
	L	21	-59	-4	-4	3.01	2.85	0.92	29
Inferior temporal gyrus	R	19	54	-68	-3	3.66	3.39	0.92	47
Precuneus	R	19	30	-78	35	3.39	3.17	1.03	51
	R	7	24	-51	42	3.32	3.11	0.99	74
Middle occipital gyrus	L	19	-33	-88	16	3.11	2.93	0.93	42
Lingual gyrus	R	17	24	-88	0	3.06	2.89	0.92	21
Posterior Cingulate gyrus	L	30	-15	-53	9	3.15	2.97	0.97	32
	R	23	12	-29	24	3.08	2.91	0.93	11
Parahippocampal gyrus	R	30	15	-45	3	3.23	3.03	0.98	49
Putamen[b]	L	N/A	18	11	-5	4.28	3.88	1.28	42
Putamen[b]	R	N/A	-15	8	-2	4.03	3.69	1.23	49
Thalamus	R	N/A	21	-12	18	3.92	3.60	1.19	60
Medial dorsal nucleus	R	N/A	9	-18	7	3.27	3.07	1.00	23

Type of incentive and level of uncertainty interactions

We first examined the interaction between financial condition and level of uncertainty. Interestingly, the results revealed activity in the caudate body (Z = 2.95). Following the behavioral results that showed a change in response to high uncertainty and financial incentive, we examined the effect of high vs. low uncertainty when no financial pressure influenced the participant's decision ([Neutral_High vs. Neutral_Low]). The dorsal ACC demonstrated enhanced activity (Figure 7.A) as did several frontal areas, including DLPFC and precentral gyrus (Table 3.A). Consistent with the analysis of the main effect of high uncertainty, occipital and parietal regions also showed enhanced activity. The opposite contrast ([Neutral_Low vs. Neutral_High]) showed no significant effects.

We then examined the areas responsive to uncertainty in the financially motivated condition ([Financial_High vs. Financial_Low]). A first obvious result was the cortical activity pattern revealed by this contrast in comparison to the effect of uncertainty without financial pressure. These regions included ventral ACC, putamen (Figure 7.B), caudate body, thalamus and brainstem (Table 3.B). The opposite contrast ([Financial_Low vs. Financial_High]) revealed no significant effects.

Finally, the examination of the financial vs. no financial incentive during conditions of high uncertainty ([Financial_High vs. Neutral_High]) revealed less activity in comparison to high vs. low uncertainty in the neutral condition. This analysis revealed several regions important to visual attention (visual cortex and pulvinar) and one moderate focus in the superior frontal gyrus (Table 3.C).

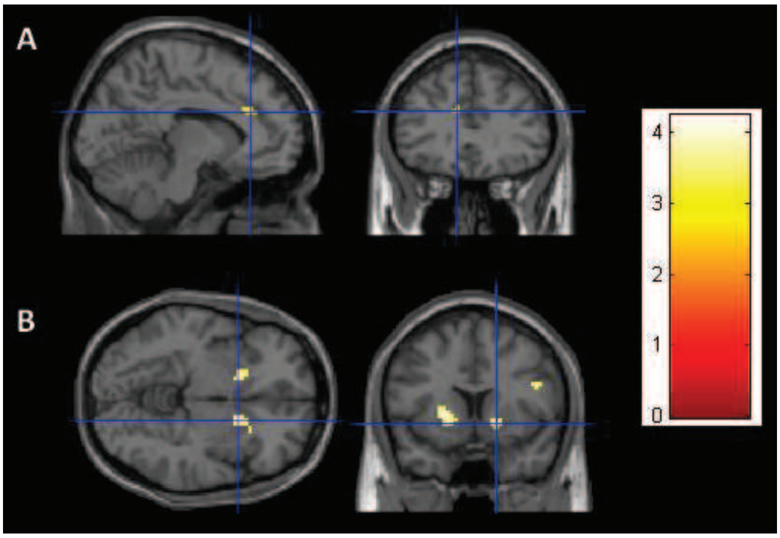

Figure 7. Effects of high vs. low uncertainty during neutral incentive, activity in the dorsal ACC (survived SVC, $p < 0.05$ FWE). (B) Effects of high vs. low uncertainty during financial incentive, activity in the putamen (survived SVC, $p < 0.05$ FWE).

Table 3. (A) Effects of high vs. low uncertainty during neutral incentive; (B) Effects of high vs. low uncertainty during financial incentive; (C) Effects of financial vs. neutral incentive under high uncertainty. Peaks occurring in clusters of ten or more contiguous voxels ($p < 0.005$ uncorrected) are reported. [a]Cohen's D measure of effect size. [b]Survived SVC ($p < 0.05$ FWE).

Brain regions	**Side**	**BA**	**Talairach Coordinates**			***t*-Score**	**z**	**Effect size[a]**	**k**
			x	y	z				
(A) High vs. low uncertainty during neutral incentive									
Inferior frontal gyrus (DLPFC)	R	9	48	15	25	3.13	2.95	0.93	26
Superior frontal gyrus	R	6	24	8	53	3.27	3.07	0.98	15
Middle frontal gyrus	L	10	-33	47	18	3.53	3.29	1.04	11
Anterior cingulate gyrus	R	24	3	0	29	2.95	2.80	0.89	17
Anterior cingulate gyrus[b]	L	32	-18	10	47	4.10	3.74	1.24	78
	L	32	-9	32	21	3.17	2.98	0.95	11
Precentral gyrus	L	6	-33	3	23	3.99	3.65	1.21	179
Inferior parietal lobule	L	40	-39	-31	36	3.71	3.43	1.08	60
Superior temporal gyrus	R	22	60	5	-7	3.19	3.00	0.97	17
	R	19	45	-79	21	2.98	2.82	0.67	19
Precuneus	L	7	-24	-63	37	3.60	3.34	1.08	66
Precuneus	L	7	-21	-51	45	3.57	3.32	1.05	13
Precuneus[b]	R	19	30	-81	35	4.24	3.84	1.27	80
Claustrum	L	N/A	-21	20	14	3.33	3.12	0.99	12
Caudate body	R	N/A	12	17	11	3.24	3.04	0.99	13
(B) High vs. low uncertainty during financial incentive									
Middle frontal gyrus (DLPFC)	L	9	-27	21	30	3.40	3.18	0.83	10
	L	46	-42	30	24	3.34	3.13	1.01	27
	R	9	48	15	22	3.22	3.03	0.96	19
Anterior cingulate gyrus	R	24	9	21	25	3.26	3.06	0.96	10
Putamen[b]	L	N/A	-18	13	-2	3.34	3.13	1.00	33
Putamen[b]	R	N/A	18	11	-5	3.43	3.20	1.02	21
Caudate body[b]	L	N/A	-9	23	11	3.47	3.24	1.06	94
Thalamus	R	N/A	21	-15	7	3.30	3.10	0.99	14
Brainstem	R	N/A	3	-32	-33	3.37	3.15	1.01	23
(C) Effects of financial vs. neutral incentive under high uncertainty									
Superior frontal gyrus	L	10	-30	60	-2	3.34	3.12	1.01	10
Middle occipital gyrus	R	19	50	-71	-6	3.18	3.00	0.87	22
Lingual gyrus	L	19	-27	-59	-1	3.00	2.84	0.90	11
Lingual gyrus	L	18	-21	-94	-5	3.71	3.43	1.09	51
Cuneus	R	18	27	-97	1	3.25	3.06	0.92	21
Pulvinar	L	N/A	-3	-33	8	3.33	3.12	1.01	57

Neural activity associations with d' discriminability index

To explore relationships between brain activity sample effect sizes and behavior, we identified the brain regions related to participants' discriminability index d' when decision making was performed under conditions of high uncertainty and financial incentive ([Financial_High]). Notably, this analysis revealed a positive correlation with DLPFC activity as well as middle frontal gyrus, post central gyrus and visual cortex (Figure 8.A and Table

4.A). Figure 8.B illustrates the association between activity parameter estimates in right DLPFC during the financial incentive with high uncertainty condition and individual d' discriminability index measures. To avoid issues related to test non-independence, we averaged the activity level in the high uncertainty condition with the financial incentive across all ROI voxels in the right DLPFC (BA9) for each participant using MarsBaR (Brett, Anton, Valabregue, & Poline, 2002), not only the voxels shown to be correlated with d' in the previous brain behavior correlation analysis. No significant negative correlations were observed.

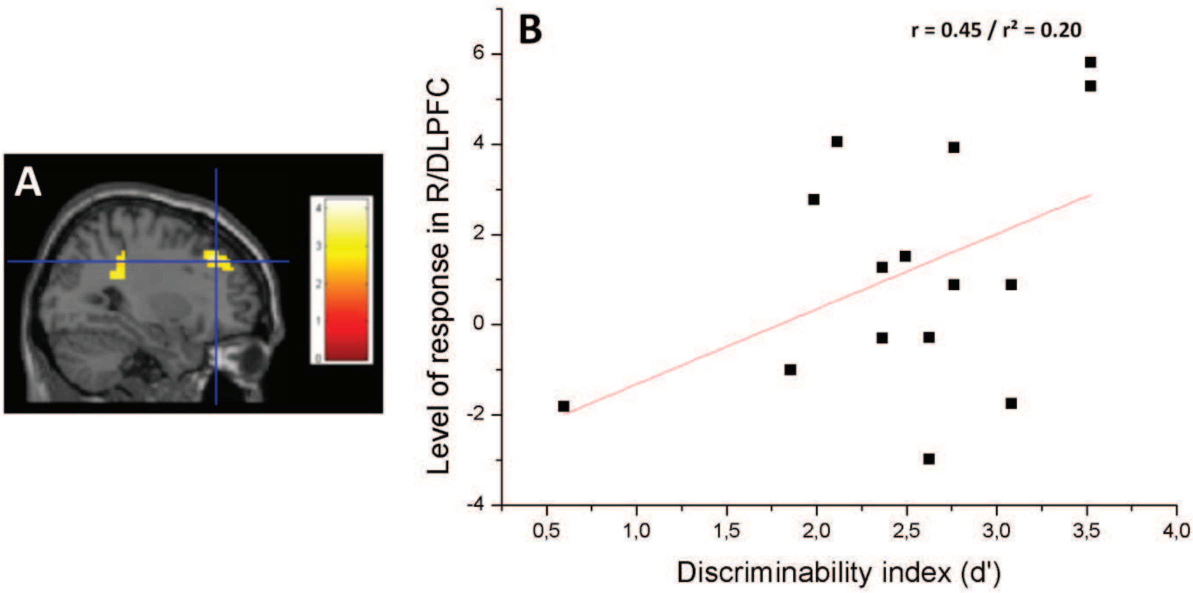

Figure 8. (A) Association between the right DLPFC (BA9) activity and participants'd' discriminability index during the financial incentive with high uncertainty condition. Results survived SVC, $p < 0.05$ FWE. (B) Illustration of the association between the average response in the right DLPFC region (BA9) for each participant with their individual d' discriminability index.

Table 4. fMRI correlations with individual d'. Peaks occurring in clusters of ten or more contiguous voxels ($p <$ 0.005 uncorrected) are reported. [a]Cohen's D measure of effect size. [b]Survived SVC ($p < 0.05$ FWE).

Brain regions	**Side**	**BA**	**Talairach Coordinates**			***t*-Score**	**z**	**Effect size[a]**	**k**
			x	**y**	**z**				
(B) Positive correlation with discriminability index (d')									
Superior frontal gyrus	L	11	-36	45	-14	3.76	3.04	2.04	12
Superior frontal gyrus (DLPFC)[b]	R	9	18	44	29	4.77	3.56	2.59	139
	R	6	39	7	42	4.68	3.52	2.51	14
Middle frontal Gyrus	R	47	48	42	-6	4.21	3.28	2.27	36
Supramarginal gyrus	L	40	-59	-49	28	4.63	3.50	2.45	24
	R	40	27	-37	30	4.22	3.29	1.95	37
Postcentral gyrus	L	3	-62	-11	24	4.42	3.39	2.32	81
Middle temporal gyrus	L	37	-45	-59	-1	3.47	2.87	1.86	12
	R	20	53	-39	-7	4.51	3.44	2.19	21
Superior occipital gyrus	R	19	42	-78	32	5.30	3.80	2.41	18
Precuneus	L	7	-18	-74	46	4.35	3.36	2.30	25
Cuneus	L	19	-12	-78	32	3.59	2.94	1.97	15
	L	17	-21	-85	8	3.40	2.83	1.86	15

4. Discussion

Our experiment was designed to explore the neural mechanisms underlying pilots' tendency to land despite bad landing conditions. We investigated the impact of economic pressure, namely the cost of a go-around, on risk taking during a plausible landing decision situation. In this experiment, both uncertainty and incentive type were manipulated. Our assumption was that pilots frame their decision to continue landing in terms of potential losses, such as money spent or fuel consumption (O' Hare & Smitheram, 1995). The results tend to confirm the intuition that a risky decision to land may be explained by a shift in decision-making criteria. Cold reasoning appeared to be more analytic and objective whereas hot reasoning was associated with a search for reward at the expense of safety. Importantly, several regions were correlated with an important index of participants' behavior, the discriminability index d'.

The decision task modulates activity in brain regions involved in high level cognitive and emotion processing

Did our novel task successfully reproduce the mental demands associated by typical landing situations? Indeed, the particular landing phase we examined is known to elicit the highest workload during a flight (Lee & Liu, 2003). As revealed by the task effect analysis (Table 1, Figure 5), the decision conditions we used provoked recruitment of the DLPFC and the ACC, two key prefrontal regions associated with various functions such as cognitive control, task monitoring, executive functions (Qin, et al., 2009) or error detection (Garavan, Ross, Murphy, Roche, & Stein, 2002). This critical point allowed us to extrapolate our results to complex real life activities, because effects of emotion on cognition seem to be particularly strong for high level cognitive functions engaged during complex decision making involving prefrontal cortex (Schoofs, et al., 2008). Our results are consistent with cardiovascular measurements obtained in a separate experiment using the same task, where the mean heart rate was significantly higher during task performance in comparison to the resting state (Causse, Baracat, Pastor, & Dehais, 2011), suggesting that the task generated notable energy mobilization and increased mental effort. Interestingly, the ACC has also been implicated in driver's decision making (Callan, Osu, Yamagishi, Callan, & Inoue, 2009), in which recruitment of this region was seen when participants were engaged in resolving uncertainty during risky driving decision making. This study sheds additional light on the role of ACC processes in our simulated aviation task. In addition, the insula is also known to be involved in decision-making under uncertainty (Singer, Critchley, & Preuschoff, 2009) and seems necessary for advantageous decision-making under risk (Weller, Levin, Shiv, & Bechara, 2009). Finally, the prominent activity increases in occipital cortex with peaks in the middle occipital gyrus and the cuneus were expected given the high visual load generated by the task and its associated strong visual-spatial modulation of primary visual cortical areas (Martinez, et al., 1999). In this sense, the study of Kéri, Decety, Roland & Gulyás (2004) had previously demonstrated that the cuneus is engaged during visual discrimination tasks with uncertainty.

Effects of the high level of uncertainty

The uncertainty level manipulation generated two types of decision-making. When the rhombi positions were non-ambiguous, all participants reported that the decision was straightforward. In contrast, when the rhombi positions were ambiguous, the participants tried to find a decision rule in a sustained way. These assertions were supported by the observed longer RTs when the ambiguity was high. These results were predictable and suggest that low uncertainty stimuli were easily categorized and that high uncertainty stimuli tended to provoke more difficult decision making.

Consistent with the behavioral results, the neuroimaging results (Figure 6, Table 2) suggest that, in the high uncertainty condition, the task was very demanding and required deeper analysis of the stimuli. Indeed the analysis of the main effect of uncertainty showed activity increases in the DLPFC (BA9), an area known to be responsive to increases in mental workload (Ayaz et al., 2012). The activity observed in the putamen confirms the central role of this area in decision making under uncertainty (Platt & Huettel, 2008). This recruitment of both the DLPFC and the putamen likely reflected engagement of a prefrontal-subcortical loop known to be triggered by decision-making under uncertainty (Onge, Stopper, Zahm, & Floresco).

Financial incentive and uncertainty: the shift from cold to hot decision making

We examined which regions were more active during hot versus cold decision-making in an uncertain context. The behavioral results confirmed that participants coped differently with the two situations. Whereas high uncertainty stimuli triggered the deepest reasoning, as they led to increased reaction times, when the high uncertainty condition was combined with financial pressure, the participants showed a shift towards hot decision-making. First, reaction times were dramatically reduced, suggesting a lower depth of reasoning before decision-making. Second, the participants clearly changed their response criteria in favor of economic optimization as they made more risky decisions to avoid the risk of a penalty in the case of a go-around. This behavior led the participants to a disruption of their discriminability performances and provoked more « crashes » (false alarm). This association of financial pressure and high uncertainty was a determining factor contributing to increased risk taking in our participants. These results were quite comparable of those seen in the neuroeconomics study conducted by Taylor et al. (2004) where monetary incentive and task complexity negatively influenced short-term memory and increased the number of false item recognitions.

A prominent neuroimaging result in our study was the drastic decrease in active cortical regions when the high uncertainty was combined with financial incentive ([Financial_High vs. Financial_Low]) (Table 3.B) in comparison to the effect of high uncertainty in the neutral context ([Neutral_High vs. Neutral_Low]) (Figure 7, Table 3.A). We notably found foci of activity in the putamen and in the caudate body. A study of Critchley et al. (2005) indicated that the caudate body activity predicts the observed degree of heart rate increase in response to emotional stimuli. Coherently, the separate experiment using the same task revealed that the maximum heart rate occurred when the uncertainty was high and the reward administered (Causse, Baracat, et al., 2011).

Interestingly, the condition associated with high uncertainty when no financial pressure influenced participant's decisions elicited enhanced activity in the dorsal "cognitive" subdivision of the ACC (BA 32) (Bush, et al., 2000). This region has been reported to be active in interference tasks (Taylor, Kornblum, Minoshima, Oliver, & Koeppe, 1994), inhibition processes (Derbyshire, Vogt, & Jones, 1998), the detection of conflict (Carter & Van Veen, 2007) and the processing of conflicts between competing information streams by sensory and/or response selection (Bush et al., 1998). This analysis of the effect of high uncertainty in a neutral context also revealed enhanced activity in the precuneus (BA19), which was not the case when uncertainty was combined to the financial incentive. This can be reasonably interpreted as an increase in top-down regulation resulting in enhanced effort with respect to visual attention. A growing number of studies suggest that early visual processing is not only affected by low level perceptual attributes, but also by higher order cognitive factors such as attention or emotion (Crockford, Goodyear, Edwards, Quickfall, & El-Guebaly, 2005; Rauss, Pourtois, Vuilleumier, & Schwartz, 2012). Consistently, Melloni et al. (2012) indicate that this type of bottom-up saliency and top-down control regulation may arise from interactions with early visual cortex (V1 to hV4).

In agreement with the prominent decrease in the number of active cortical regions when high uncertainty was combined with the financial incentive in comparison to the effect of high uncertainty in the neutral condition, contrasting the financial vs. no financial incentive conditions in the context of high uncertainty (Table 3.C) revealed fewer regions in comparison to the high uncertainty in the neutral context (Table 3.A). No activity survived SVC. This outcome brings additional evidence in favor of a disruption of rational decision making and a change toward hot decision-making when participants simultaneously faced high uncertainty and biased financial incentive.

Given the variability in participant response profiles, a key goal of our study was to examine regions that exhibited associations with participants' decision-making strategies (conservative – cold decision maker - vs. liberal – hot decision maker) when participants were exposed to both the financial payoff and maximum levels of uncertainty. Most notably, the right DLPFC was positively associated with the individual d' discriminability index (Figure 8, Table 4). This result showed that this related high level cognition region was less recruited by participants demonstrating poor discriminability in response to the financial incentive. It is very likely that participants who choose to accept landing more frequently were influenced by the better mathematical expectancy related to this decision. This change in response criteria provoked a shift from cold to hot decision making. The sustained reasoning associated with uncertainty, as revealed by frontal activity, was transformed into a straightforward economical preprogrammed response strategy, notably resulting in right DLPFC deactivations. This result tends to confirm the study of Fecteau et al. (2007) that demonstrated that participants receiving transcranial direct stimulation of DLPFC adopted a risk-averse response style during ambiguous decision making. In the same way, Knoch et al. (2006) showed that disruption of right DLPFC by low-frequency repetitive transcranial magnetic stimulation induces risk-taking behavior. Finally, whereas we expected OFC activity, it is worth noting that the examination of negative associations revealed no effects in this region. It suggests that the observed disruptive effect of reward and uncertainty on discriminability performance is mainly provoked by deactivation of several key frontal cortical regions (*i.e.* DLPFC, ACC), rather than by a strong deleterious emotional influence that would have likely generated OFC activations (Bechara, Damasio, & Damasio, 2000; Kringelbach, 2005; Coricelli, et al., 2005: Li et al., 2009).

The current study has some limitations that deserve attention. First, the rather small sample size (n = 15) may have resulted in identification of effects unique to this particular cohort. In addition, small samples tend to have lower statistical power and are therefore more likely to identify only strong task effects. Due to the difficulty of recruiting experienced pilots, our participants were non-pilots. However, our previous experiment using the same tasks (Causse, Baracat, et al., 2011) included 19 pilots who demonstrated a similar behavioral pattern, notably an increased number of landing acceptances during the financially motivated condition when uncertainty was high. This similar behavior between pilots and non-pilots in reaction to financial incentive and uncertainty demonstrates the typical occurrence of the mechanism that produces plan continuation error and emphasizes that all people may be particularly risk seeking when faced with the prospect of losses (Kahneman & Tversky, 1979). Finally, before recruitment, participants had a brief interview conducted by a trained psychologist, but no specific screening concerning the presence or absence of psychiatric disorders. Future studies should include more rigorous clinical experimental control with respect to the presence or absence of psychiatric disorders, estimated using structured instruments such as the Mini International Neuropsychiatric Interview (MINI) (Sheehan et al., 1998).

Despite the above limitations, given the reduced reaction time, the change in response behavior, and our neuroimaging results, we conclude that the co-occurrence of high uncertainty and the administration of reward provoked a disruption of rational reasoning vs. economical reasoning, inducing a change in participant's motivation from safety constraints to economical ones. This shift from cold to hot reasoning offers interesting theoretical prospects for aviation safety. PCE could be the result of different aversive negative consequences associated with the go-around decision, such as the financial cost for the company. The present study confirms the current translational research interest in merging cognitive neurosciences with cognitive ergonomics (Sarter & Sarter, 2003), within a neuroergonomics approach (Parasuraman, 2003), allowing identification of the underlying mechanisms of human error such as PCE.

5. Conclusion

We examined the neural mechanisms involved in decision-making performed under variations in financial incentive and situational uncertainty. Our study incorporated a combination of functional neuroimaging with an ecologically valid task performed routinely by airline pilots during the landing phase of a flight.

Though the economical consequences of this task were not comparable with actual flight conditions, the payoff matrix we employed was designed to reproduce the negative consequences linked with the decision to go-around in a manner efficient enough to provoke risky behavior such as PCE. Indeed, it incited our volunteers to maximize their monetary reward and biased their response criterion from safety to economic considerations in spite of the fact that all participants were told that, as in real life, taking into account flight safety was essential in this experiment. Combined with behavioral outcomes, our neuroimaging results revealed a shift from cold to hot decision-making in response to uncertainty when financial incentive was present. Whereas a large network of key frontal regions, including DLPFC and ACC, was observed in response to uncertainty, a different collection, not including these frontal regions, was found when biased financial incentive was combined with uncertainty. Participants with poor decision-making performance (lower d') who adopted more risky behavior demonstrated lower activity in the right DLPFC. This interesting outcome demonstrates that reward and uncertainty can temporarily jeopardize rational decision making during complex ecologically valid tasks.

Acknowledgements

The authors would like to thank Olivier Dufor, Rodolphe Nénert, Sébastien Scannella for their assistance in data analysis as well as Jonathan Levy for helpful feedback on prior drafts of this manuscript.

References

Adamson, M. M., Samarina, V., Xiangyan, X., Huynh, V., Kennedy, Q., Weiner, M. (2010). The impact of brain size on pilot performance varies with aviation training and years of education. *Journal of the International Neuropsychological Society, 16*(3), 412-423.

Ayaz, H., Shewokis, P. A., Bunce, S., Izzetoglu, K., Willems, B., & Onaral, B. (2012). Optical brain monitoring for operator training and mental workload assessment. *NeuroImage, 59*(1), 36-47.

Bechara, A., Damasio, H., & Damasio, A. R. (2000). Emotion, decision making and the orbitofrontal cortex. *Cerebral Cortex, 10*(3), 295-307.

Brett, M., Anton, J. L., Valabregue, R., & Poline, J. B. (2002). Region of interest analysis using the MarsBar toolbox for SPM 99. *NeuroImage, 16*, S497.

Bush, G., Luu, P., & Posner, M. I. (2000). Cognitive and emotional influences in anterior cingulate cortex. *Trends in cognitive sciences, 4*(6), 215-222.

Bush, G., Whalen, P. J., Rosen, B. R., Jenike, M. A., McInerney, S. C., & Rauch, S. L. (1998). The counting Stroop: an interference task specialized for functional neuroimaging—validation study with functional MRI. *Human Brain Mapping, 6*(4), 270-282.

Caldwell, J. A., Mu, Q., Smith, J. K., Mishory, A., Caldwell, J. L., Peters, G. (2005). Are Individual Differences in Fatigue Vulnerability Related to Baseline Differences in Cortical Activation? *Behavioral neuroscience, 119*(3), 694.

Callan, A. M., Osu, R., Yamagishi, Y., Callan, D. E., & Inoue, N. (2009). Neural correlates of resolving uncertainty in driver's decision making. *Human brain mapping, 30*(9), 2804-2812.

Callan, D. E., Gamez, M., Cassel, D. B., Terzibas, C., Callan, A., Kawato, M., et al. (2012). Dynamic Visuomotor Transformation Involved with Remote Flying of a Plane Utilizes the 'Mirror Neuron' System. *PloS one, 7*(4). doi: 10.1371/journal.pone.0033873

Carter, C. S., & Van Veen, V. (2007). Anterior cingulate cortex and conflict detection: an update of theory and data. *Cognitive, Affective, & Behavioral Neuroscience, 7*(4), 367-379.

Causse, M., Baracat, B., Pastor, J., & Dehais, F. (2011). Reward and Uncertainty Favor Risky Decision-Making in Pilots: Evidence from Cardiovascular and Oculometric Measurements. *Applied Psychophysiology and Biofeedback, 36*(4), 231-242.

Causse, M., Dehais, F., Arexis, M., & Pastor, J. (2011). Cognitive aging and flight performances in general aviation pilots. *Aging, Neuropsychology, and Cognition, 18*(5), 544-561.

Causse, M., Dehais, F., & Pastor, J. (2011). Executive functions and pilot characteristics predict flight simulator performance in general aviation pilots. *The International Journal of Aviation Psychology, 21*(3), 217-234.

Coricelli, G., Critchley, H. D., Joffily, M., O'Doherty, J. P., Sirigu, A., & Dolan, R. J. (2005). Regret and its avoidance: a neuroimaging study of choice behavior. *Nature neuroscience, 8*(9), 1255-1262.

Critchley, H. D., Rotshtein, P., Nagai, Y., O'Doherty, J., Mathias, C. J., & Dolan, R. J. (2005). Activity in the human brain predicting differential heart rate responses to emotional facial expressions. *NeuroImage, 24*(3), 751-762.

Crockford, D. N., Goodyear, B., Edwards, J., Quickfall, J., & El-Guebaly, N. (2005). Cue-induced brain activity in pathological gamblers. *Biological psychiatry, 58*(10), 787-795.

Damasio, A. (1994). *Descartes' error: Emotion, reason, and the human brain*: New York: Grosset/Putnam.

Derbyshire, S., Vogt, B., & Jones, A. (1998). Pain and Stroop interference tasks activate separate processing modules in anterior cingulate cortex. *Experimental Brain Research, 118*(1), 52-60.

Dreher, J. C., Kohn, P., & Berman, K. F. (2006). Neural coding of distinct statistical properties of reward information in humans. *Cerebral Cortex, 16*(4), 561.

Fecteau, S., Pascual-Leone, A., Zald, D. H., Liguori, P., ThÃ©oret, H., Boggio, P. S. (2007). Activation of prefrontal cortex by transcranial direct current stimulation reduces appetite for risk during ambiguous decision making. *The Journal of neuroscience, 27*(23), 6212-6218.

Fossati, A., Di Ceglie, A., Acquarini, E., & Barratt, E. S. (2001). Psychometric properties of an Italian version of the Barratt Impulsiveness Scale 11 (BIS 11) in nonclinical subjects. *Journal of clinical psychology, 57*(6), 815-828.

Garavan, H., Ross, T., Murphy, K., Roche, R., & Stein, E. (2002). Dissociable executive functions in the dynamic control of behavior: inhibition, error detection, and correction. *Neuroimage, 17*(4), 1820-1829.

Goel, V., & Dolan, R. (2003). Reciprocal neural response within lateral and ventral medial prefrontal cortex during hot and cold reasoning. *Neuroimage, 20*(4), 2314-2321.

Goh, J., & Wiegmann, D. (2002). Human factors analysis of accidents involving visual flight rules flight into adverse weather. *Aviation, space, and environmental medicine, 73*(8), 817.

Kahneman, D., & Tversky, A. (1979). Prospect theory: An analysis of decision under risk. *Econometrica: Journal of the Econometric Society*, 263-291.

Kéri, S., Decety, J., Roland, P. E., & Gulyás, B. (2004). Feature uncertainty activates anterior cingulate cortex. *Human brain mapping, 21*(1), 26-33.

Knoch, D., Gianotti, L. R. R., Pascual-Leone, A., Treyer, V., Regard, M., Hohmann, M. (2006). Disruption of right prefrontal cortex by low-frequency repetitive transcranial magnetic stimulation induces risk-taking behavior. *The Journal of neuroscience, 26*(24), 6469-6472.

Kringelbach, M. L. (2005). The human orbitofrontal cortex: linking reward to hedonic experience. *Nature Reviews Neuroscience, 6*(9), 691-702.

Lancaster, J. L., Tordesillasâ€• GutiÃ©rrez, D., Martinez, M., Salinas, F., Evans, A., Zilles, K. (2007). Bias between MNI and Talairach coordinates analyzed using the ICBMâ€• 152 brain template. *Human Brain Mapping, 28*(11), 1194-1205.

Lancaster, J. L., Woldorff, M. G., Parsons, L. M., Liotti, M., Freitas, C. S., Rainey, L. (2000). Automated Talairach atlas labels for functional brain mapping. *Human Brain Mapping, 10*(3), 120-131.

Lee, Y., & Liu, B. (2003). Inflight workload assessment: Comparison of subjective and physiological measurements. *Aviation, Space and Environmental Medicine, 74*(10), 1078-1084.

Li, C. R., Chao, H. H. A., & Lee, T. W. (2009). Neural correlates of speeded as compared with delayed responses in a stop signal task: an indirect analog of risk taking and association with an anxiety trait. *Cerebral Cortex, 19*(4), 839.

Maldjian, J. A., Laurienti, P. J., Kraft, R. A., & Burdette, J. H. (2003). An automated method for neuroanatomic and cytoarchitectonic atlas-based interrogation of fMRI data sets. *NeuroImage, 19*(3), 1233-1239.

Martinez, A., Anllo-Vento, L., Sereno, M. I., Frank, L. R., Buxton, R. B., Dubowitz, D., et al. (1999). Involvement of striate and extrastriate visual cortical areas in spatial attention. *Nature neuroscience, 2*, 364-369.

Melloni, L., van Leeuwen, S., Alink, A., & Muller, N. G. (2012). Interaction between Bottom-up Saliency and Top-down Control: How Saliency Maps Are Created in the Human Brain. *Cerebral Cortex*. doi: 10.1093/cercor/bhr384

Menda, J., Hing, J. T., Ayaz, H., Shewokis, P. A., Izzetoglu, K., Onaral, B. (2011). Optical Brain Imaging to Enhance UAV Operator Training, Evaluation, and Interface Development. *Journal of intelligent & robotic systems*, 1-21.

Nance, J. (1986). Blind trust: How deregulation has jeopardized airline safety and what you can do about it. *W. Morrow and Co., New York*.

O' Hare, D., & Smitheram, T. (1995). "Pressing on" into deteriorating conditions: An application of behavioral decision theory to pilot decision making. *The International Journal of Aviation Psychology, 5*(4), 351-370.

Onge, J. R. S., Stopper, C. M., Zahm, D. S., & Floresco, S. B. Separate Prefrontal-Subcortical Circuits Mediate Different Components of Risk-Based Decision Making. *The Journal of neuroscience, 32*(8), 2886-2899.

Orasanu, J., Ames, N., Martin, L., & Davison, J. (2001). Factors in Aviation Accidents: Decision Errors. *Linking expertise and naturalistic decision making*, 209.

Parasuraman, R. (2003). Neuroergonomics: Research and practice. *Theoretical Issues in Ergonomics Science, 4*(1), 5-20.

Peres, M., Van De Moortele, P. F., Pierard, C., Lehericy, S., Satabin, P., Le Bihan, D. (2000). Functional magnetic resonance imaging of mental strategy in a simulated aviation performance task. *Aviation, space, and environmental medicine, 71*(12), 1218-1231.

Platt, M. L., & Huettel, S. A. (2008). Risky business: the neuroeconomics of decision making under uncertainty. *Nature neuroscience, 11*(4), 398-403.

Qin, S., Hermans, E. J., van Marle, H. J. F., Luo, J., & Fernández, G. (2009). Acute psychological stress reduces working memory-related activity in the dorsolateral prefrontal cortex. *Biological psychiatry, 66*(1), 25-32.

Rauss, K., Pourtois, G., Vuilleumier, P., & Schwartz, S. (2012). Effects of attentional load on early visual processing depend on stimulus timing. *Human brain mapping, 33*(1), 63-74.

Rhoda, D., & Pawlak, M. (1999). An assessment of thunderstorm penetrations and deviations by commercial aircraft in the terminal area. *Massachusetts Institute of Technology, Lincoln Laboratory, Project Report NASA/A-2, 3*.

Sarter, N., & Sarter, M. (2003). Neuroergonomics: opportunities and challenges of merging cognitive neuroscience with cognitive ergonomics. *Theoretical issues in ergonomics science, 4*(1), 142-150.

Schaefer, A., Colette, F., Philippot, P., Van der Linden, M., Laureys, S., Delfiore, G. D. (2003). Neural correlates of “hot” and “cold” emotional processing: a multilevel approach to the functional anatomy of emotion. *NeuroImage, 18*, 938-949.

Schoofs, D., Preuss, D., & Wolf, O. T. (2008). Psychosocial stress induces working memory impairments in an n-back paradigm. *Psychoneuroendocrinology, 33*(5), 643-653.

Sheehan, D. V., Lecrubier, Y., Sheehan, K. H., Amorim, P., Janavs, J., Weiller, E. (1998). The Mini-International Neuropsychiatric Interview (MINI): the development and validation of a structured diagnostic psychiatric interview for DSM-IV and ICD-10. *Journal of clinical psychiatry, 59*, 22-33.

Singer, T., Critchley, H. D., & Preuschoff, K. (2009). A common role of insula in feelings, empathy and uncertainty. *Trends in cognitive sciences, 13*(8), 334-340.

Spielberger, C., Pedrabissi, L., & Santinello, M. (1996). STAI, state-trait anxiety inventory, forma y: manuale. *Firenze: OS Organizzazioni Speciali*.

Taylor, S. F., Kornblum, S., Minoshima, S., Oliver, L. M., & Koeppe, R. A. (1994). Changes in medial cortical blood flow with a stimulus-response compatibility task. *Neuropsychologia, 32*(2), 249-255.

Taylor, S. F., Welsh, R. C., Wager, T. D., Luan Phan, K., Fitzgerald, K. D., & Gehring, W. J. (2004). A functional neuroimaging study of motivation and executive function. *Neuroimage, 21*(3), 1045-1054.

Vul, E., & Kanwisher, N. (2010). Begging the question: The non-independence error in fMRI data analysis. *Foundational issues for human brain mapping*, 71-91.

Weller, J. A., Levin, I. P., Shiv, B., & Bechara, A. (2009). The effects of insula damage on decision-making for risky gains and losses. *Social neuroscience, 4*(4), 347-358.